Charge modulations in La_2CuO_4-based cuprates

L.-M. Peng,* M. Gao, and Z. F. Dong
Beijing Laboratory of Electron Microscopy, Institute of Physics and Center for Condensed Matter Physics, Chinese Academy of Sciences, P.O. Box 2724, 100080 Beijing, People's Republic of China

X. L. Dong, B. R. Zhao, and Z. X. Zhao
National Laboratory for Superconductivity, Institute of Physics and Center for Condensed Matter Physics, Chinese Academy of Sciences, 100080 Beijing, People's Republic of China

(Received 1 November 1999; revised manuscript received 13 January 2000)

Electron microscopy experiments reveal that in a Cu-rich polycrystalline $La_2CuO_{4.003}$, grains may phase separate into hole-rich and hole-poor grains at room temperature and in a hole-rich crystalline grain, holes are distributed inhomogeneously over a distance that is smaller than 500 nm. In a hole-rich grain it is shown that hole modulation superlattice reflections may be induced by electron beam, and the size of the modulation domain is estimated to be around 150 nm. The observed modulation superlattice reflections are shown to result from hole localization around a set of parallel modulation planes that are inclined to the CuO_2 planes. When intersecting with a CuO_2 plane, holes lying on and close to the set of modulation planes form a two-dimensional hole stripe pattern on the CuO_2 plane. It is suggested that the observed static hole stripes result from the pinning of fluctuating stripes by electron-beam induced effects. Our results indicate that holes associated with the same modulation plane but different CuO_2 planes are strongly correlated and interlayer hole interaction is not in general negligible.

I. INTRODUCTION

Copper oxide superconductors are obtained by adding charge carriers into ''parent'' compounds that are antiferromagnetic (AF) insulators. At sufficiently low temperature, long-range AF order develops in which there is an unpaired spin on each copper ion pointing in a direction that alternates from site to site. Upon doping the charge-carriers introduced into the CuO_2 layers destroy the long-range AF order rapidly, and the compounds become superconductors beyond a critical carrier concentration.[1] Many recent experiments show that even in the superconducting state, local AF correlations exist,[2–4] and the simplest way to understand the coexistence of local antiferromagnetism with homogeneous superconductivity is in terms of spatial segregation of the doped charges.[5,6] If the segregated charges in high-T_c superconductors form stripes, then these charges can move around in these materials more freely.[7] At lower temperature, local AF spin order develops in the domains between the charge stripes. Extensive neutron-scattering experiments have been carried out successfully to investigate the static as well as fluctuating spin correlations.[8] Studies of charge ordering (which drives spin ordering) using the technique of neutron diffraction are, however, not as direct and successful as that of spin correlations. This is because neutrons do not scatter from the charge directly. In this paper we will show that the technique of electron diffraction may be used efficiently for studying hole stripes in La_2CuO_4-based cuprates.

In an earlier study,[9] we showed, using transmission electron microscope (TEM), that a Cu-rich high-T_c superconducting $La_2CuO_{4.003}$ sample may phase separate into modulated and unmodulated phases. These microscopic observations agree well with magnetization measurements that show that there exist in the sample one superconducting phase with $T_c \approx 35$ K and an antiferromagnetic phase with $T_N \approx 244$K. Upon annealing in a flowing Ar gas at 800 °C for 8 h, the superconductivity of the sample disappeared together with the modulated phase. These results, as well as some other recent experiments,[4,10,11] seem to suggest that static stripes and therefore magnetic ordering and superconductivity may coexist in the same sample,[12] on the contrary to the belief that static charge stripes should kill superconductivity rather than promote it. In this letter we report a direct TEM observation of the formation and characteristics of static hole stripes in Cu-rich La_2CuO_4 materials, and show that our observations are consistent with the idea that the observed static stripes result from pinning of dynamical fluctuating stripes.

II. EXPERIMENT

The Cu-rich $La_2CuO_{4+\delta}$ samples used in this study were polycrystalline samples that were prepared using the conventional solid-state reaction method.[9] All electron-energy-loss spectroscopy (EELS) and high-resolution electron microscopy (HREM) experiments were performed using a Philips CM200/FEG (200 keV) electron microscope equipped with a double tilt cold stage and a Gatan imaging filter. Some of the diffraction experiments involving large tilting angles were performed using a Philips CM12 (120 keV) electron microscope. The excess oxygen content δ of our samples was determined to be 0.003 using gas effusion spectra method.[9,13]

III. RESULTS AND DISCUSSIONS

Two Cu-rich $La_{2-x}Cu_{1+x}O_{4.003}$ samples with nominal atomic ratios of La:Cu=2:1.06 and 2:1.18 were investigated. These two nominal ratios correspond to values of $x=0.058$

and $x=0.113$, respectively. Detailed diffraction and EELS observations show that in the samples, a second phase of CuO (which exhibits distinct electron diffraction patterns and EELS near edge structures and may be unambiguously identified) coexists with the main La-Cu-O phase.[14] The number of grains with the CuO phase is, however, much smaller than that with the La-Cu-O phase. HREM imaging of the La-Cu-O grains reveals that these grains are well crystallites with an almost perfect La_2CuO_4 lattice, while EELS analysis of the grains shows that these grains contain a higher concentration of Cu than that found in a usual $La_2CuO_{4+\delta}$ sample. These results show that some excess Cu atoms have been intercalated into the La-Cu-O lattice homogeneously. These excess Cu atoms might stay either in the interstitial sites or replace La ions lying in between the CuO_2 planes, in analogy with the compounds $La_{2-x}Sr_xCuO_4$ and $La_{2-x}Ba_xCuO_4$.[1] If the excess Cu ions were staying at the interstitial sites, these ions would likely to be in the Cu^{2+} ionic state losing electrons and reducing the hole content in the sample. In principle these excess electrons provided by the interstitial Cu ions could be accommodated by excess oxygen ions lying also at the interstitial sites, but this would require a rather high excess oxygen content, i.e., $\delta > x \approx 0.11$, and this is known not to be true for our samples. EELS analysis reveals that our samples are p type (see below), suggesting that the excess Cu ions contribute holes rather than electrons as they usually do. This is possible only if the excess Cu^{2+} ions replace La^{3+} ions and therefore contribute effectively one hole for every such replacement. Alternatively, all Cu atoms might be accommodated on the CuO_2 planes, leaving some vacancies at the La sites in between the CuO_2 planes so that the overall atomic La:Cu ratio may be less than 2:1 as in our samples. We expect, however, that the vacancy model would result in higher strain energy than the model in which Cu ions substitute La ions. In a previous study,[9] we showed via magnetization measurements (Fig. 1 in Ref. 9) that in a Cu-rich $La_2CuO_{4+\delta}$ sample, the antiferromagnetic interaction is stronger than in a usual $La_2CuO_{4+\delta}$ sample. This result is also not expected from the vacancy model but it is consistent with the picture that the excess Cu^{2+} ion with a spin of 1/2, substitutes the site of the La^{3+} ion with no spin, so that the antiferromagnetic exchange interaction between CuO_2 planes is enhanced. Assuming that the excess Cu replaces La, our EELS results shown that about 5% La ions were replaced by the excess Cu ions. This value is close to what one would expect from the nominal value of $x=0.113$ and indicates that only a small amount of excess Cu atoms have been accommodated in the CuO phase as mentioned above.[14]

Figure 1(a) shows a bright-field image of a sample with nominal value $x=0.113$. Four grains (with grain boundaries marked by white-dotted line) of the size of a few microns, are clearly visible. The quality of the crystallites was verified by HREM imaging, and shown in Fig. 1(b) is an example of HREM images obtained from the circled area of grain 1 [see Fig. 1(a)]. Image simulations confirm that the brighter rows of spots in Fig. 1(b) correspond to the [110] projections of the CuO_2 layers, and the less bright rows between the brighter rows correspond to $(LaO)_2$ layers. Selected area electron diffraction (SAED) from the grains shown in Fig. 1(a), reveals that they all have La_2CuO_4 lattice, and a typical

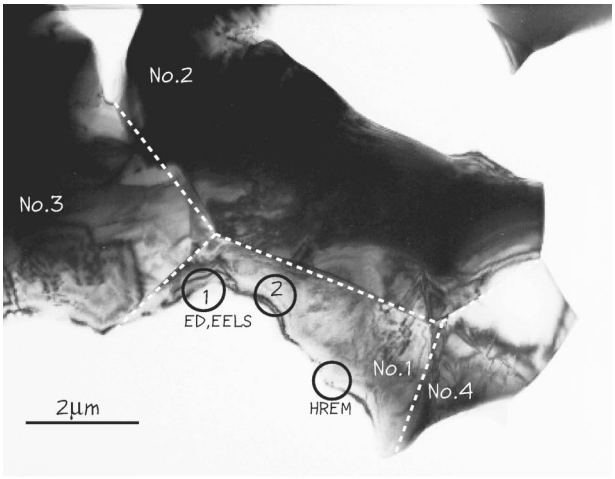

(a)

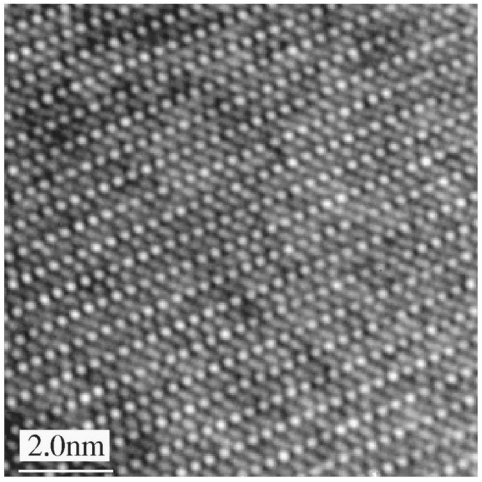

(b)

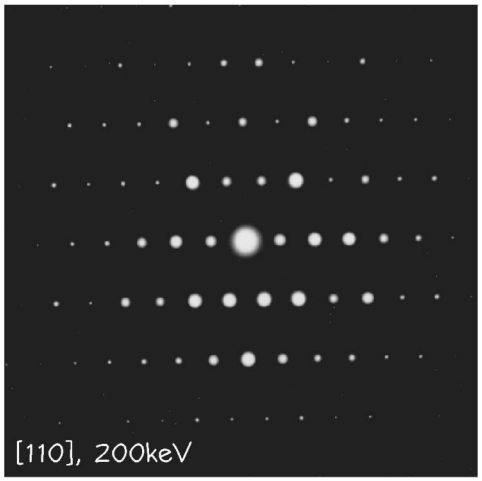

(c)

FIG. 1. (a) A bright-field image taken from a polycrystalline $La_{1.82}Cu_{1.18}O_{4.003}$ sample, (b) a HREM image taken from the circled area to the right of grain 1, and (c) a typical diffraction pattern taken from the circled area to the left of grain 1. All observations were made near the [110] zone axis using 200 keV.

room temperature (RT) SAED pattern obtained from grain 1 is shown in Fig. 1(c). Notably no diffraction pattern obtained from the sample shows superlattice reflections, i.e., no static modulation exists in the sample.

Microscopically whether a sample has phase separated

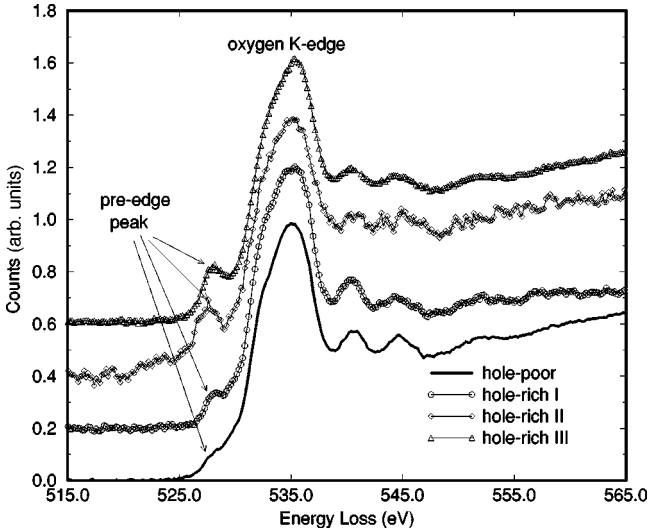

FIG. 2. EELS spectra taken from hole-poor grain 3 and three different regions in grain 1 of Fig. 1(a) for 200-keV primary beam energy and a near [110] zone axis incidence.

into a hole-rich phase and a hole-poor phase may be verified using EELS.[15] Shown in Fig. 2 are some oxygen *K*-edge EELS spectra measured at RT using 200 keV primary beam energy. The solid curve near the bottom of Fig. 2 was obtained from grain 3, and other spectra were obtained from grain 1 of Fig. 1(a). These spectra show that near the main oxygen absorption *K* edge at 532 eV there exists a small pre-edge peak at approximately 528 eV. For lightly doped samples this pre-edge peak corresponds to transitions of electrons from the occupied oxygen 1*s* core level into the charge-transfer band (dominated by the oxygen 2*p* orbitals). Detailed calculations based on a one-band Hubbard model[16] and comparison with x-ray absorption spectra of $La_{2-x}Sr_xCuO_4$ (Ref. 17) show that the integrated pre- edge peak intensity increases monotonically with increasing hole concentration on the CuO_2 planes. The intensity of the pre-edge peak near 528 eV may therefore be regarded as a measure of the local hole concentration. In all experiments the diameter of the selected area aperture used is about 500 nm. Since the aperture was usually placed near the edge of the specimen as indicated in Fig. 1(a), the dimension of the selected specimen area contributing to EELS spectra was typically of the size of 200 to 300 nm. Our EELS results demonstrate that at RT a polycrystalline Cu-rich sample with $x = 0.113$ has phase separated into hole-rich grains (such as grains 1 and 2) and hole-poor grains (such as grains 3 and 4). Within a single hole-rich grain (such as grain 1) holes are distributed inhomgeneously over a distance not longer than 500 nm, i.e., a single crystalline grain may phase separate into phases with different hole concentration.

As shown in Fig. 1(c), initial diffraction from the grains shown in Fig. 1(a) resulted in only fundamental Bragg reflections, regardless of the hole concentration of the illuminated grain. At this stage one definite statement that one may make regarding these grains is that there exists no static modulation in these grains. One cannot rule out, however, that there exists dynamic ordering in the grains, i.e., ordering that changes with time. This is because what one observes in an electron microscope is principally a time-averaged electrostatic potential. Rapidly varying ordering cannot therefore be shown up in an electron-diffraction pattern or in an image that takes usually from a fractional second to a few seconds to record. Prolonged examinations of hole-poor grains did not reveal any new features, i.e., these grains remain hole poor and result in only fundamental Bragg reflections.

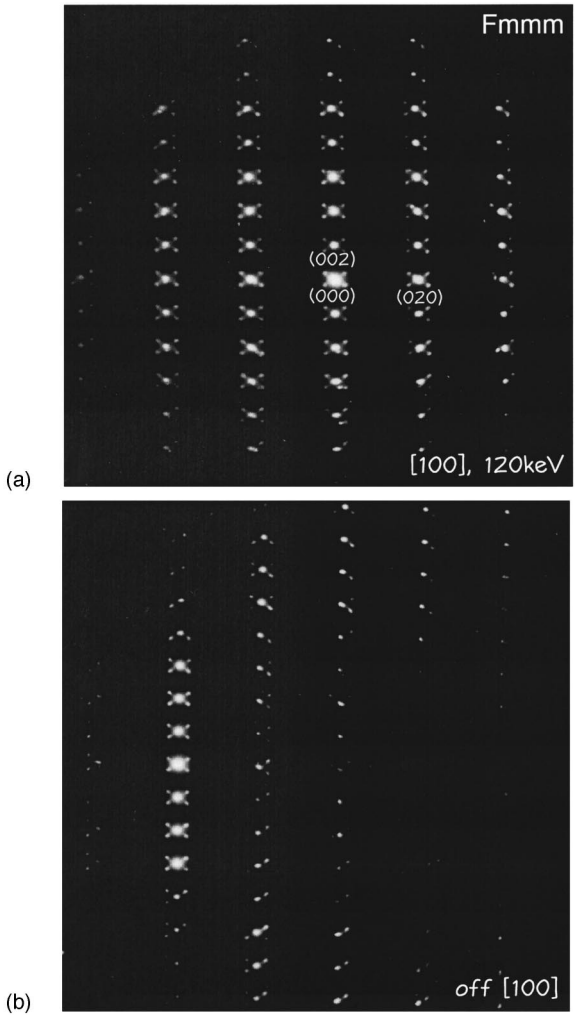

FIG. 3. (a) A [100] zone axis electron diffraction pattern and (b) a diffraction pattern obtained for a tilted incidence. Both diffraction patterns were obtained from grain 1 of Fig. 1(a) and for a 120-keV primary beam energy.

Hole-rich grains behaved very differently. Take a hole rich grain, such as grain 1 of Fig. 1(a), for an example. After continuous illumination under the electron-beam modulation superlattice reflections gradually appeared in diffraction patterns taken from the grain and the intensity of the superlattice reflections reached a maximum after a few minutes of observation and remained stable under electron beam. An example of so obtained SAED patterns from grain 1 at RT is shown in Fig. 3(a). Well-defined superlattice reflections are clearly visible. To verify the nature of the modulation, diffraction patterns from different orientations and tilts were recorded and a pattern obtained for a tilted incidence near [100] zone axis is shown in Fig. 3(b). These experiments show that the RT modulation wave vectors are of the form $\mathbf{q} \approx 0.057\langle 0 \ \pm 4 \ 6\rangle = \pm 0.23\mathbf{b}^* + 0.35\mathbf{c}^*$, and that the modulation is basically compositional modulation (see be-

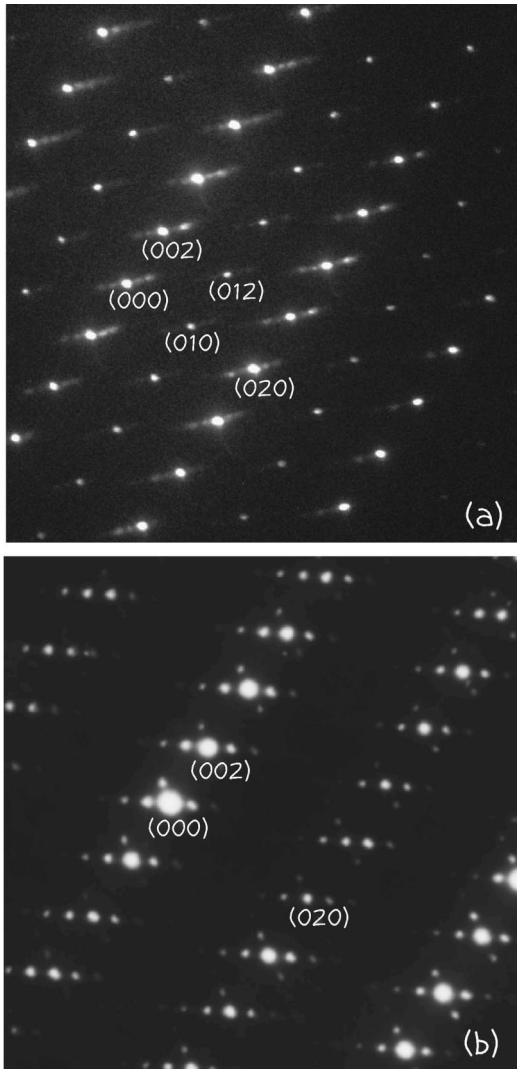

FIG. 4. Transmission electron-diffraction patterns taken from a Cu-rich sample $La_{2-x}Cu_{1+x}O_{4+\delta}$ with a nominal value $x=0.058$ for a primary beam energy of 200 keV at (a) room temperature and (b) 93 K.

low). We note that these modulation superlattice reflections may result from either two types of twin domains or a single type of domain with a superposition of two sets of modulations. For the later case, we would expect to see a two-dimensional net of superlattice reflections and this is incompatible with our observations at lower temperatures [see Fig. 4(b)]. We have used a selected area aperture of the size of 150 nm for searching single domain. Although diffraction patterns dominated by one set of one-dimensional superlattice reflections may sometimes be observed, usually two sets such superlattice reflections coexist. We conclude therefore that the domain size is typically not bigger than 150 nm. In what follows we shall be concerned only with the basic superlattice reflection of the type $\mathbf{q}=0.23\mathbf{b}^*+0.35\mathbf{c}^*$. Experiments have also been performed at temperatures between RT and 93 K. The modulation wave vector was found to be not sensitive to temperature variations. Throughout our experiments the hole concentration, as revealed by EELS spectra from the same region, remained high as long as the modulation superlattice reflections remained bright. After tens of minutes exposure to intense electron beam the intensities of the modulation superlattice reflections were found to diminish and the space group of the lattice was found to change from *Fmmm* to *Bmab*. EELS spectrum from a corresponding grain revealed that the grain had became hole poor after the transformation. These observations demonstrate that the superlattice reflections are closely related to the hole concentration in the grain. We may conclude here, therefore, that the modulation that results in superlattice reflections is hole related.

The transformation of the lattice symmetry from *Fmmm* to *Bmab* may be understood as resulting from the reduction of local hole content. Originally a RT La_2CuO_4 lattice favors a *Bmab* symmetry that differs from a *Fmmm* symmetry principally in the ordering of the tilt of the CuO_6 octahedrons. The tile of the CuO_6 octahedrons is caused by the mismatch between the Cu-O-Cu (larger) and La-O-La (smaller) bond lengths in the CuO_2 and $(LaO)_2$ layers. With additional holes being added onto the CuO_2 planes, the Cu-O-Cu bond length decreases and so does the tilt of the CuO_6 octahedrons, leading eventually to a *Fmmm* symmetry. This is the symmetry exhibited in Figs. 3(a), 3(b), and 4(b). It should be noted that a perfect match between Cu-O-Cu and La-O-La bond lengths is practically impossible since local hole concentration is not uniform across the sample and these bonds respond to thermal vibrations differently. In general, finite thermal vibrations of ions, especially those oxygen ions on the CuO_2 planes, tend to randomize the tilts of the CuO_6 octahedrons. Macroscopic ordering of the tilts of the CuO_6 octahedrons may only be destroyed when the Cu-O-Cu chain is nearly straight, i.e., when the bond angle is near 180°. A corollary is that when the local hole concentration is high, as may result from electronic phase separation and high level of hole doping, the local lattice will exhibit *Fmmm* symmetry. On the other hand, when the doping level is lower and phase separation is not thorough, the local structure will exhibit *Bmab* symmetry as shown in Fig. 4(a) for $x=0.058$ and RT. As the temperature decreases, phase separation becomes more thorough [as evidenced in Fig. 4(b), which shows that comparing with RT superlattice reflections shown in Fig. 3(a), the lower temperature superlattice reflections are sharper and better defined, and higher-order superlattice reflections begin to appear], and the lattice symmetry becomes *Fmmm*.

The observations of samples with lower nominal value $x=0.058$ differ from that shown in Figs. 2 and 3 for samples with $x=0.113$ also in several other aspects. First, the RT modulation superlattice reflections shown in Fig. 3(a) are sharper and better defined than that shown in Fig. 4(a) for $x=0.058$. This result is consistent with our earlier suggestion that the AF exchange interaction is enhanced by the introduction of excess Cu^{2+} ions with spin 1/2 between the CuO_2 layers.[18] Second, the basic modulation wave vector for the lower value of $x=0.058$, changes with varying temperature. Figure 4(a) shows that for the sample with $x=0.058$ the basic RT modulation wave vector $\mathbf{q}$ is approximately $0.048\langle 0\ 4\ 10\rangle$, while the corresponding vector $\mathbf{q}=0.041\langle 0\ 6\ 8\rangle$ at 93 K [Fig. 4(b)]. It should be pointed out that at both RT and 93 K the magnitude of $\mathbf{q}$ equals 0.05 Å^{-1}. In the light of a recent discovery[4] that a linear relation exists between the incommensurability of the spin fluctuations and effective hole concentration, we may specu-

late that a similar relation exists between hole concentration and $|\mathbf{q}|$. Our results then suggest that hole concentration remains approximately the same during temperature experiments and that the tilting of $\mathbf{q}$ direction results mainly from temperature variation rather than hole concentration.

We now consider what caused the superlattice reflections. Consider first the intercalated copper ions between the CuO_2 layers. We note that these ions are immobile at temperatures below RT, the observed superlattice reflections that changed with decreasing temperature cannot therefore result from ordering of these ions. In principle, oxygen vacancies might exhibit ordered structure resulting in shear planes and superlattice reflections.[19] The existence of an appreciable amount of oxygen vacancies inevitably means, however, that the sample would be electron rich rather than hole rich as evidenced by our EELS observations (Fig. 2). The interstitial oxygen ions, located between two adjacent LaO layers, could also be a cause for the observed superlattice reflections, as in the case of $La_2NiO_{4+\delta}$.[20] This model, however, cannot account for our observations consistently. First, it should be noted that the excess oxygen content $\delta=0.003$ in our sample is about three times less than the threshold value of $\delta=0.01$ for a $La_2CuO_{4+\delta}$ sample to phase separate. It is therefore not clear whether long-range ordering between excess oxygen ions would develop in our sample with $\delta=0.003$. Second, our Cu-rich samples with $x=0.113$, exhibit *Fmmm* symmetry at all temperatures below RT [see Figs. 3(a) and 3(b)], indicating that the structure has, on average, no ordered tilting of CuO_6 octahedrons. The antiphase domain boundary model proposed for accommodating interstitial oxygen ions[3] therefore does not apply in our sample. Third, interstitial oxygen ions between the $(LaO)_2$ planes, introduce local lattice distortion, notably to the four apical oxygen neighbors.[21] Ordering of the interstitial oxygen ions would inevitably lead to a modulation with a considerable displacive component. The tilted electron diffraction pattern shown in Fig. 3(b) suggests, however, that the modulation is largely composition or valence modulation. Any appreciable displacive component of the modulation would manifest itself most strongly in higher-order reflections and show angular characteristics, both features are absent in Fig. 3(b). In what follows we will outline a model based on hole ordering, and

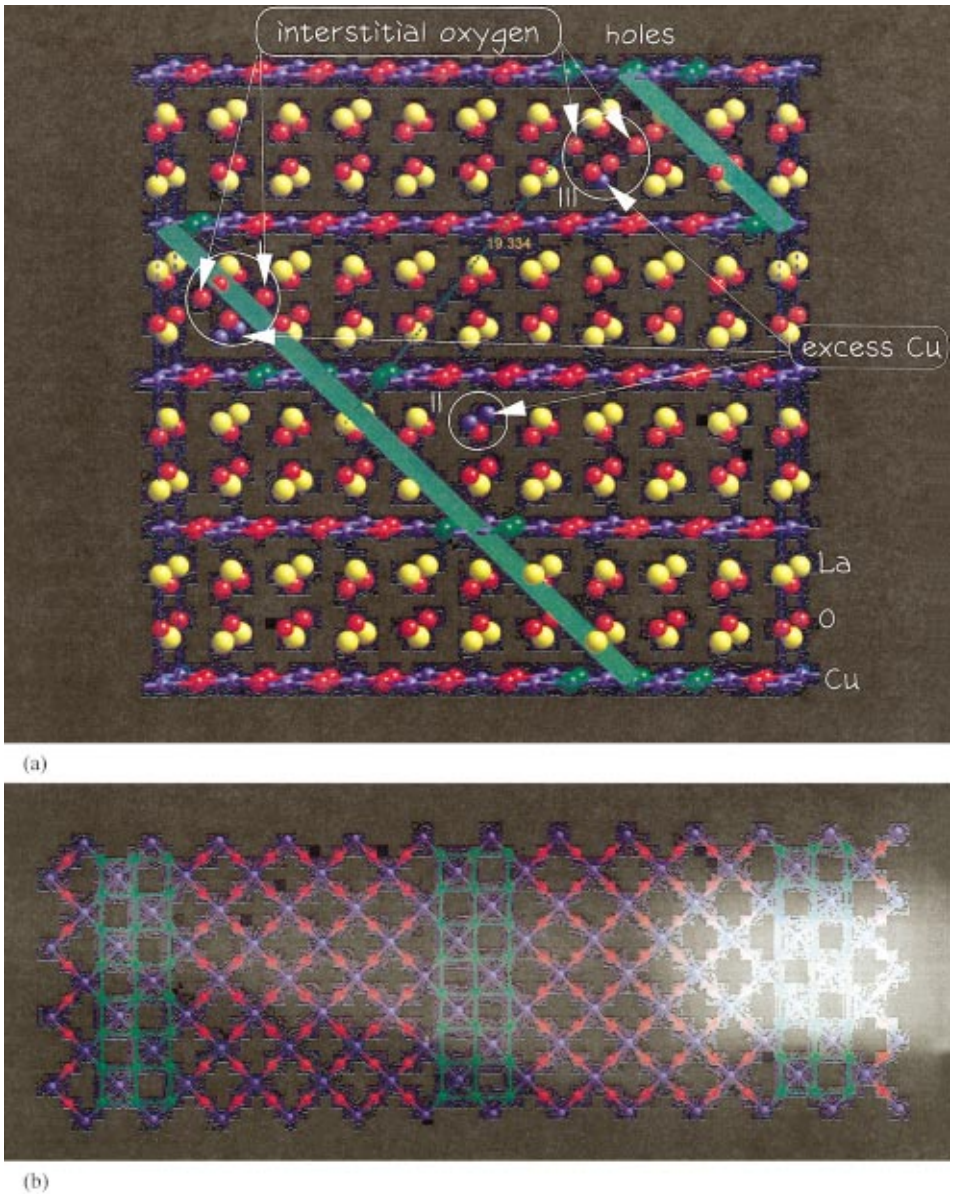

FIG. 5. (Color) A model for a hole modulated $La_{2-x}Cu_{1+x}O_{4+\delta}$ lattice: (a) a three-dimensional view of the model, (b) a [001] top view of a single CuO_2 layer showing hole stripes.

show that this model may account for all our observations consistently.

A hole interacts strongly with incident high-energy electrons via electrostatic potential, and a simple model for this interaction is the screened Coulomb potential

$$\varphi(r)=\frac{e^2}{r}\exp(-r/a),$$

where a is the effective screen length. To a first-order approximation the electron scattering amplitude by the hole is given by the Fourier transform of the potential $\varphi(\mathbf{r})$, giving

$$A(\mathbf{q})=\frac{1}{2\pi^2}\frac{e^2a^2}{1+a^2q^2}.$$

For a large screen length, we have $A(q)\approx e^2/(2\pi^2q^2)$. This expression clearly shows that for a zero value of q, the scattering amplitude diverges, and strong diffraction effects are expected for modulation structures involving small values of q.

To model holes on the CuO_2 planes, we take an ionic view and regard a hole as a replacement of an O^{2-} ion on the CuO_2 planes by an O^{1-} ion, and this model is consistent with the fact that the charge-transfer band below the Fermi level of a La_2CuO_4 crystal is dominated by the oxygen $2p$ orbitals.[17,16] Shown in Fig. 5(a) is a model of a hole modulated $La_{2-x}Cu_{1+x}O_{4+\delta}$ crystal with $\mathbf{q}=0.048\langle 0\ 4\ 10\rangle$ (corresponding roughly to the RT modulation of a sample with $x=0.058$). The figure shows that the corresponding modulation planes in real space are indeed inclined to the CuO_2 plane. Unlike spin stripes, which give only first order superlattice peaks,[22] higher-order hole superlattice reflections develop rapidly at temperatures below RT [see Fig. 4(b), the intensity ratio between the second-order superlattice reflection to the first order is 0.8 for (002) and 0.72 for (004) reflections]. We therefore modeled the hole-rich modulating planes with relatively narrow width. When these modulation planes intersect with a particular CuO_2 layer, a typical hole stripes pattern[5,6] is produced as shown in Fig. 5(b). Dynamical electron diffraction simulation using the multislice method[23] is shown in Fig. 6. Qualitatively the simulated diffraction pattern agrees well with experimental patterns.

If one believes that dynamical charge and spin stripe existed in a hole-rich grain prior to our examinations, Figs. 3(a) and 3(b) may then be understood to result from the pinning of fluctuating hole stripes by electron-beam induced effects. The fact that the static modulation planes observed in the sample with $x=0.113$ are less mobile than that with $x=0.058$, suggests that the intercalated Cu ions must play an important role in pinning down the fluctuating hole stripes. Also suggestive is the fact that electron beam increases, among other things, the mobility of interstitial oxygen ions. One model that accounts for all our observations on the Cu-rich $La_2CuO_{4+\delta}$ samples is shown in Fig. 5(a) and the basic features may be summarized as follows: (1) the excess oxygen atoms take the form of O^{2-} and occupy interstitial sites between the $(LaO)_2$ layers, (2) the excess or intercalated Cu atoms take the form of Cu^{2+} and replace La^{3+} ions, (3) each intercalated Cu^{2+} ion sitting at one of the La^{3+} sites may be effectively regarded as a negative charge embedded in a uniform background of charges. Since the radius of the Cu^{2+} ion is smaller than that of the La^{3+} ion, the replacement of La^{3+} ions by Cu^{2+} ions produces larger and therefore favorable interstitial spaces around the intercalated Cu^{2+} ions than around the La^{3+} ions for accommodating interstitial oxygen ions. (4) The intercalated Cu^{2+} and interstitial oxygen ions were initially distributed in the crystal homogeneously. These effective ''single'' negative charges do not have sufficient strength to pin down the meandering hole stripes. (5) Upon electron-beam irradiation the interstitial oxygen ions become more mobile and some of them may find favorable interstitial spaces around the intercalated Cu^{2+} ions and form ''negatively charged clusters'' around the Cu^{2+} ions. These negatively charged clusters may serve as pinning centers and provide stronger dragging force on the positively charged hole stripes compared with the homogeneously distributed single negative charges. In samples with more intercalated Cu^{2+} ions, such as the samples with $x=0.113$, there exist more effective pinning centers (AF exchange interaction between CuO_2 layers is also stronger) than that with less intercalated Cu^{2+} ions, such as the sample with $x=0.058$. The pinned static hole stripes in the sample with more intercalated Cu^{2+} ions, therefore, appear to be less mobile than that with less intercalated Cu^{2+} ions. In Fig. 5(a) there is shown three clusters of ''negatively charged'' particles around the hole modulation planes. These centers are not regularly distributed since the intercalated Cu^{2+} ions are not.

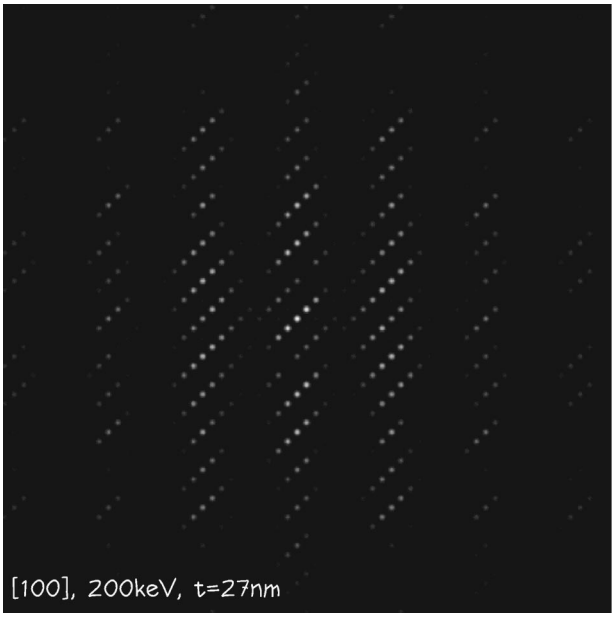

FIG. 6. Simulated [100] electron-diffraction pattern for a crystal thickness of 270 Å and a primary beam energy of 200 keV. The $La_{2-x}Cu_{1+x}O_{4+\delta}$ crystal is assumed to be of *Fmmm* symmetry, the modulation period 19.334 Å, and wave vector pointing along $\langle 0\ 4\ 10\rangle$.

Our experimental results show that in a hole-rich grain, holes are distributed around some parallel modulation planes that are inclined to the CuO_2 planes. When intersecting with a particular CuO_2 plane, holes lying on and close to the modulation planes, form a two-dimensional stripe pattern on the CuO_2 plane. While holes belonging to the same stripe or different stripes that are associated with the same modulation

plane are strongly correlated, those lying on the same CuO_2 plane but belonging to different stripes and therefore different modulation planes, may be less strongly correlated, i.e., the interplane hole interaction may be comparable to the intraplane interaction in contrast to the magnetic exchange interaction. The width of the stripes on the CuO_2 plane decreases as the temperature decreases, i.e., holes become more localized around the modulation planes at lower temperature. This is evidenced in Fig. 4, which shows that higher-order superlattice reflections are clearly visible in the diffraction pattern taken at lower temperature [Fig. 4(b)] but not seen in the diffraction pattern taken at RT [Fig. 4(a)]. This indicates that the modulation plane becomes sharper and better defined at lower temperature, and holes become more localized around the modulation planes as temperature decreases.

IV. SUMMARY

In a polycrystalline Cu-rich $La_{2-x}Cu_{1+x}O_{4+\delta}$ sample, grains have been observed to phase separate into hole-rich and hole-poor grains, and in a hole-rich grain holes have been observed to distribute inhomogeneously across the crystallite. Hole related superlattice reflections have been observed in hole-rich grains and shown to result from hole localization on planes that are inclined to the CuO_2 planes. For lightly doped samples with $x=0.058$, the modulation wave vector was observed to depend on temperature. Our results suggest that holes situating on the same modulation plane but different CuO_2 planes are strongly correlated. Temperature experiments show that holes become more localized around the modulation planes as temperature decreases, suggesting an increasing interaction between holes localizing around the same modulation plane but lying on different CuO_2 planes as temperature decreases.

ACKNOWLEDGMENTS

This work was supported by the National Science Foundation of China and the Chinese Academy of Sciences. The authors would like to thank Professor R. H. Wang and Dr. W. Zhou for valuable discussions.

*Also at Department of Electronics, Peking University, Beijing 1000871, China.

[1] C.P. Poole, H.A. Farach, and R.J. Creswick, *Superconductivity* (Academic Press, New York, 1995).
[2] J.M. Tranquada, B.J. Sternlieb, J.D. Axe, Y. Nakamura, and S. Uchida, Nature (London) **375**, 561 (1995).
[3] B.O. Wells, Y.S. Lee, M.A. Kastner, R.J. Christianson, R.J. Birgeneau, K. Yamada, Y. Endoh, and G. Shirane, Science **277**, 1067 (1997).
[4] K. Yamada, C.H. Lee, K. Kurahashi, J. Wada, S. Wakimoto, S. Ueki, H. Kimura, Y. Endoh, S. Hosoya, R.J. Birgeneau, M. Greven, M.A. Kastner, and Y.J. Kim, Phys. Rev. B **57**, 6165 (1998).
[5] V.J. Emery and S.A. Kivelson, Physica C **209**, 597 (1993).
[6] V.J. Emery and S.A. Kivelson, Physica C **263**, 44 (1996).
[7] V.J. Emery, S.A. Kivelson, and J.M. Tranquada, Proc. Natl. Acad. Sci. USA **96**, 8814 (1999).
[8] J.M. Tranquada, N. Ichikawa, K. Kakurai, and S. Uchida, J. Phys. Chem. Solids **60**, 1019 (1999).
[9] X.L. Dong, Z.F. Dong, B.R. Zhao, Z.X. Zhao, X.F. Duan, L.-M. Peng, W.W. Huang, B. Xu, Y.Z. Zhang, S.Q. Guo, L.H. Zhao, and L. Li, Phys. Rev. Lett. **80**, 2701 (1998).
[10] A.W. Hunt, P.M. Singer, K.R. Thurber, and T. Imai, Phys. Rev. Lett. **82**, 4300 (1999).
[11] Y.S. Lee, R.J. Birgeneau, M.A. Kastner, Y. Endoh, S. Wakimoto, K. Yamada, R.W. Erwin, S.H. Lee, and G. Shirane, Phys. Rev. B **60**, 3643 (1999).
[12] R.F. Service, Science **283**, 1106 (1999).
[13] Z.G. Li, H.H. Feng, Z.Y. Yang, A. Hamed, S.T. Ting, and P.H. Hor, Phys. Rev. Lett. **77**, 5413 (1996).
[14] M. Gao, L. -M. Peng, X. L. Dong, B. R. Zhao, G. D. Liu, and Z. X. Zhao (unpublished).
[15] Z.F. Dong, L.-M. Peng, X.F. Duan, X.L. Dong, B.R. Zhao, Z.X. Zhao, J. Yuan, and R.H. Wang, Phys. Rev. B **59**, 3489 (1999).
[16] M. Hybertsen, E.B. Stechel, W.M.C. Foulkes, and M. Schluter, Phys. Rev. B **45**, 10 032 (1992).
[17] C.T. Chen, F. Sette, Y. Ma, M.S. Hybertsen, E.B. Stechel, W.M.C. Foulkes, M. Schluter, S.-W. Cheong, A.S. Copper, L.W. Rupp, B. Batlogg, Y.L. Soo, Z.H. Ming, A. Krol, and Y.H. Kao, Phys. Rev. Lett. **66**, 104 (1991).
[18] X.L. Dong, B.R. Zhao, Z.X. Zhao, L. Wei, L. Zhou, B. Xu, H. Chen, G.C. Che, Y.M. Ni, B. Yin, J.W. Li, L.H. Zhao, and Z.Y. Xu, Chin. Phys. Lett. **14**, 225 (1997).
[19] G. Van Tendeloo and S. Amelinckx, Physica C **176**, 575 (1991).
[20] Z. Hiroi, T. Obata, M. Takano, Y. Bando, Y. Takeda, and O Yamamoto, Phys. Rev. B **41**, 11 665 (1990).
[21] P.G. Radaelli, J.D. Jorgensen, A.J. Schultz, B.A. Hunter, J.L. Wagner, F.C. Chou, D.C. Chou, and D.C. Johnston, Phys. Rev. B **48**, 499 (1993).
[22] J.M. Tranquada, J. Phys. Chem. Solids **59**, 2150 (1998).
[23] John M. Cowley, *Diffraction Physics*, 2nd ed. (North-Holland, Amsterdam, 1990).